

Bankline Assessment of Shibsra-Passur River by Satellite Imagery and Hydrodynamic Modeling using Delft3D

Nusaiba Afsara Haque¹, Anika Azad², Md. Khairul Amin³ and G. M. Jahid Hasan^{4*}

^{1,2,3,4}Department of Civil Engineering, Military Institute of Science and Technology (MIST), Dhaka, Bangladesh

emails: ¹nusaiba.afsara@gmail.com; ²anika4422@gmail.com; ³aminkhr21@gmail.com and ^{4*}jahid@ce.mist.ac.bd

ARTICLE INFO

Article History:

Received: 10th June 2024

Revised: 23th October 2024

Accepted: 23th October 2024

Published: 26th December 2024

Keywords:

Erosion-accretion

Satellite images

DSAS

Delft3D

Sundarbans

ABSTRACT

The Sundarbans, a prolific mangrove wetland ecosystem part of the world's largest delta formed by the Ganges, Brahmaputra, and Meghna rivers, contribute immensely to coastal stability and protection. In deltaic mangroves such as the Sundarbans, recurrent erosion and accretion caused by the transportation of unconsolidated sediments by rivers, interact with flow velocity and bed shear to generate continuous morphological dynamics. This study analyzed the bankline migration patterns of the Shibsra and Passur rivers within the Bangladesh portion of the Sundarbans using satellite images and assessed their hydrodynamic behavior by developing a two-dimensional model using Delft3D. This study utilized Landsat and Sentinel images from 2009-2021 to identify critical erosion and deposition zones applying the DSAS tool of ArcGIS. A two-dimensional hydrodynamic model was then developed and calibrated to simulate flow velocity, bed shear stress, and water levels in these critical zones. The model was validated against limited available water level data. Six critical zones were identified, with four erosion-prone and two deposition-prone areas. The model results indicated increased velocities and bed shear stresses in the erosion zones relative to non-critical areas, while the deposition zones experienced reduced velocities and bed shear stresses. The study reveals that the high values of velocity and bed shear stresses are responsible for the morphological changes of erosion, thus emphasizing the significance of close monitoring with remotely sensed images.

This work is licensed under a [Creative Commons Attribution-NonCommercial 4.0 International License](https://creativecommons.org/licenses/by-nc/4.0/)

1. INTRODUCTION

The most significant attributes of Bangladesh's rivers are aggradation, degradation or change in plan forms, changes to the river beds, and meandering characteristics (Laz, 2012). The alluvial rivers of Bangladesh are known for their morphological dynamism, as they constantly undergo erosion and sedimentation processes that lead to changes in their hydraulic geometry, plan form, and longitudinal profile (Habibullah, 1987). Any artificial or natural changes may cause a shift or break in the morphological equilibrium (Winterbottom, 2000; Petts & Gurnell, 2005). Additionally, such an imbalance can create channel instability, resulting in channel pattern alterations (Ramos & Gracia, 2012; Midha & Mathur, 2014). Natural processes for an alluvial river include bank erosion, downcutting, bank accretion etc.

Furthermore, human activities frequently impact the rate of morphological changes. Moreover, morphological

adjustments are undertaken to consider the variety of flows and sediment loads from upstream, repeatedly threatening channel stability. Since the courses of the rivers regularly changes, there are no actual permanent maps of the river bank lines (Bristow, 1987; Hassan *et al.*, 1997). Riverbank erosion is one of the most crucial problems in river morphology, which still needs continuous investigation and monitoring. When the velocity of flowing water surpasses the shearing resistance of sediments on the peripheral region of a river bank, bank erosion occurs (Nicholas, 2013a, 2013b; Das *et al.*, 2014; Ghosh & Sahu, 2018).

Geomorphological dynamics are the primary process driving the growth of the Sundarbans - the deltaic mangrove forest southwest of Bangladesh and south of West Bengal (Islam & Wahab, 2005). Previous morphological studies concentrated on detecting bankline alterations and the growth or decline of mangrove vegetation. However, such studies lacked information on

the erosion and accretion processes unique to specific channels and rivers in the Sundarbans (Uddin *et al.*, 2011). This study focuses on the Sundarbans' two major rivers, Shibsa and Passur. These rivers convey freshwater from upstream and feed many tributaries within the forest area. Increased upstream freshwater inflow abates salinity in the river system, but this effect is much less pronounced on the rivers and channels to the west (Wahid *et al.*, 2007). Moreover, presence of mangroves at the land-water transition, the drag forces generated by the trees and roots, and also the uneven mud floor influence local hydrodynamics (Mazda *et al.*, 1995; Kobashi & Mazda, 2005). Understanding and monitoring these dynamic processes, including the interplay between freshwater inflow, salinity, and mangrove vegetation, is crucial for effective river management, sustainable development, and conservation of the Sundarbans ecosystem. This comprehensive approach enables the development of effective mitigation strategies and ensures sustainable river management practices in this unique and complex environment.

Comprehending the hydrodynamics of a river surrounded by mangroves can be facilitated through numerical models that are thoroughly validated against field measurements (Abu Hanipah *et al.*, 2018). River banklines are conventionally delineated and compared using topographical maps, aerial photographs, and satellite imagery. However, software like the Digital Shoreline Analysis System (DSAS) provides quantitative, scientific, automated, and software-based models for calculating river bank erosion or deposition (Hasanuzzaman *et al.*, 2021). Developed by the United States Geological Survey (USGS), the DSAS model has been widely utilized to analyze and assess shifts in shorelines and river banks along user-defined transects (Barnard *et al.*, 2010; Bouchahma & Yan, 2014; Mahapatra *et al.*, 2014; David *et al.*, 2016; Ashraf & Shakir, 2018; Roy *et al.*, 2018; Hasan & Matin, 2019; Jana, 2019). Mathematical models enable interpolation and extrapolation in space- and time-based on field observations and an understanding of physical processes and their interactions (Laz, 2012; Sadeghi *et al.*, 2013). Consequently, well-calibrated and verified hydrodynamic models are recommended for further investigation of these potential outcomes.

Hydrodynamic and morphological assessments of rivers are crucial for understanding their actual characteristics and evolving patterns, which numerical models can analyze (Lotsari *et al.*, 2014; Nicholas, 2012). Several studies have employed a combination of different methods including visual inspection, data analysis, satellite image interpretation, mathematical modeling etc. to examine morphological changes in major rivers of Bangladesh, such as the Meghna River (Hossain, 2014), the Jamuna River (Brahmaputra) (Momen *et al.*, 2020; Laz, 2012), and the rivers in the Sundarbans mangrove forest (Sohel *et al.*, 2021; Anam *et al.*, 2021; Rahman, 2012). These studies have provided valuable insights into the meandering patterns, erosion-accretion dynamics, and bankline changes, as well as the influence of environmental factors like climate change and erosion-accretion processes.

Additionally, the Delft3D model has been employed to assess morphological changes and hydrodynamic characteristics, such as flow velocity, water level, and bed shear stress, in rivers like the Jamuna (Laz, 2012) and the Karnafuli (Alam & Matin, 2013), demonstrating the robustness of this tool for conducting morphological assessment studies in major water bodies. In this study images extracted from satellites such as Landsat and Sentinel, along with transect lines generated by DSAS, were used to identify areas prone to erosion and accretion within the Sundarbans. Additionally, a two-dimensional (2D) hydrodynamic model was developed for the Shibsa and Passur rivers. The study aims to simulate and understand various parameters that influence the rivers' morphological behavior, including velocity, bed shear stress, water level etc. from the hydrodynamic model. By combining the analysis of satellite images with hydrodynamic modeling, the study will adopt a multidisciplinary approach to gain insights into the complex dynamics of river morphology within the Sundarbans.

2. MATERIALS AND METHODS

To analyze the morphological changes occurring in the Shibsa and Passur Rivers within the Sundarbans, a combined approach involving satellite image analysis and numerical modeling was adopted. Shoreline analysis techniques were employed to quantify the bankline movement over time, while a 2D hydrodynamic model was developed to understand the hydrodynamic processes governing these morphological changes.

A. Study Area

The Sundarbans, part of the world's largest delta formed by the Ganges (Padma), Brahmaputra (Jamuna), and Meghna rivers, is home to 177 rivers that flow into the Bay of Bengal. However, this mangrove forest is continuously changing due to erosion, degradation, and deforestation. The present study focuses on the shifting bankline dynamics of two major rivers within the Sundarbans, the Shibsa and Passur rivers. The Shibsa River (22°26'48"N 89°25'46"E to 21°43'16"N 89°30'2"E) is approximately 100 km long, with about 27 km of its length flowing through the Paikgachha upazila, while the remaining course demarcates the common boundary between Paikgachha and Dacope upazilas. Inside the Sundarbans, the Shibsa meets the Passur River at Akram Point and receives various rivulets and khals from multiple directions, which enriching its flow. The Passur River (22°21'24"N 89°37'51"E to 21°43'16"N 89°30'2"E), a tributary of the Padma River, leaves the Madhumati River northeast of Khulna city and flows around 177 km southward past the port at Mongla and through the Sundarbans as an extension of the Rupsa River to the Bay of Bengal (WCMC, 2005; Giri *et al.*, 2007). Notably, The Passur (2139 ha, 55 ha/year) and Shibsa (1809 ha, 46.5 ha/year) have the highest erosion rates, while the accretion rate was significantly lower over the last four decades (1980–2019) (Sohel *et al.*, 2021). Although the Shibsa and Passur rivers are not contiguous upstream, they join downstream, as depicted in Figure 1. The consistent water depth of the Shibsa River allows transportation of boats,

large vessels, commodities, and passengers throughout the year. Most of the Passur River travels through the Sundarbans, maintaining the forest's ecosystem, and both rivers play a crucial role in sustaining the mangrove, wildlife, flora, fauna, and fish in the region.

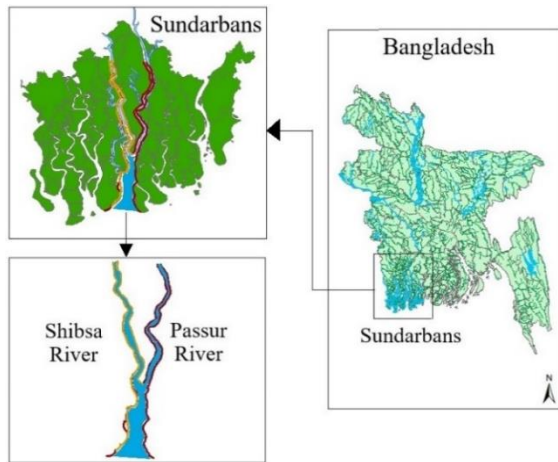


Figure 1: Shibsa and Passur Rivers passing through the Sundarbans

B. Satellite Image Analysis

In this study, Landsat and Sentinel images were utilized for analysis, and the methodology is described in the following sub-sections.

i. Collection of Satellite Images

For the analysis of river bankline movements, satellite images from Landsat-7 Enhanced Thematic Mapper Plus (ETM+) and Sentinel-2 were used. Landsat-7 ETM+, launched on 15 April 1999, provides valuable multispectral observations and has been widely used for various remote sensing applications (Markham *et al.*, 2008). On the other hand, Sentinel-2 launched on 23 June 2015, offers an overall accuracy of 5%, surpassing Landsat-7 by 4%. Earth Explorer, developed by the United States Geological

Survey (USGS), served as the primary portal for accessing publicly available satellite images.

For this study, Landsat-7 images of 2009 and 2013, and Sentinel-2 images of 2016, 2018, and 2021 were selected to analyze the movement of riverbanks of the Passur and Shibsa rivers as shown in Figure 2. The selection of images was based on the availability of clear images, resulting in irregular intervals ranging from two to four years between the chosen range of years to identify significant changes in the river banklines. The analysis considered Band 5 images, as this band can penetrate through thin clouds and distinguish the moisture content of soil and vegetation, which aids in clearly delineating banklines. Landsat-7 images have a spatial resolution of 30 meters, while Sentinel-2 has a better resolution of 20 meters, allowing for more accurate mapping of subtle features. Table 1 summarizes the bands used by different satellites and the reasons for selection for this study.

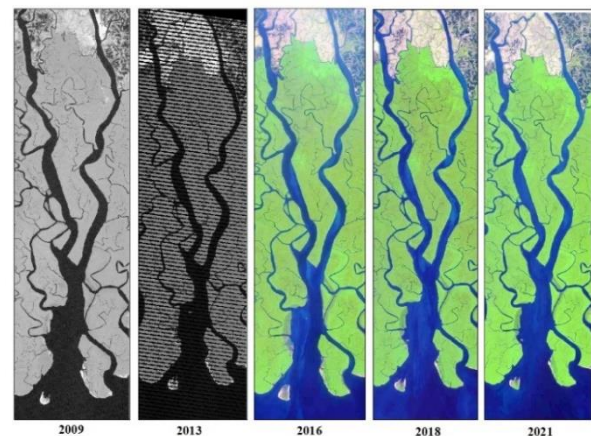


Figure 2: Satellite images of different years covering the Shibsa and Passur River. Images of years 2009 and 2013 are collected from Landsat and the remaining images are from Sentinel

Table 1

Bands used for the study to identify bank-lines

Sensor	Band No.	Band Name	Wavelength	Resolution	Reason for Consideration
Landsat-7 ETM+	Band 5	Short-Wave Infrared (SWIR 1)	1.55-1.75 μm	30 meters	B5 can penetrate thin clouds
Sentinel-2	Band 5	Visible and Near Infrared (VNIR)	0.705 μm	20 meters	B5 can differentiate between land and water effectively

ii. Bank-line Delineation using ArcGIS

To identify the banklines and understand their movement due to erosion and accretion over different years, the delineation of banklines was carried out using ArcGIS. The process involved manual digitization, which converts geographic data collected from images into vector data by tracing the features. Manual digitization was chosen over other methods due to its relatively high accuracy despite being time-consuming. The manual digitization process involved delineating the banklines on the satellite images for the considered years (i.e. 2009, 2013, 2016, 2018, and 2021) as shown in Figure 3. The digitized banklines were displayed with distinct colors for each year to better identify the bankline movement as depicted in Figure 4.

Selected locations were zoomed-in to get a clearer view of the shifting, where movements of 100 to 200 meters were observed.

iii. Digital Shoreline Analysis System (DSAS)

The DSAS software, an ESRI ArcGIS add-in, was employed to determine the bankline movement numerically, referred to as Net Bankline Movement (NBM) in this study. Transect lines were automatically generated by the DSAS with a 150-meter spacing based on the digitized banklines for the study years from 2009 to 2021. A baseline was manually drawn along the middle of the Shibsa River, representing the left and right banks as illustrated in Figure 5. DSAS then calculated the NBM

using the distance between various banklines and the baseline along the perpendicular transect lines, which ran between the baseline and the banklines closer to the land (Thieler *et al.*, 2009). The NBM was calculated as the total movement in meters between the oldest and newest bankline positions for each transect, where positive values

indicated bank movement toward the land (erosion or landward migration), and negative values indicated movement toward the river (accretion or riverward migration). The transect rates which were generated by the DSAS, automatically generates Net Shoreline Movement (NSM), which has been designated as NBM in this study.

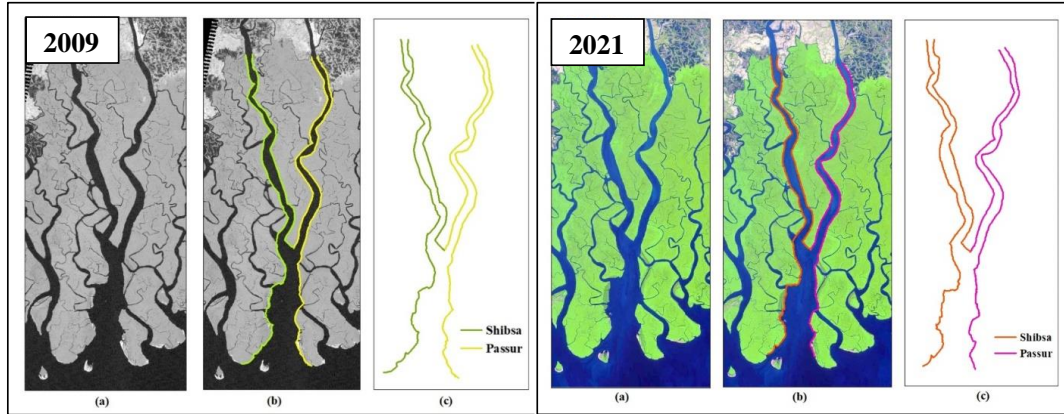


Figure 3: Manual digitization process using ArcGIS: (a) raw images of years 2009 and 2021, (b) raw images with digitized bank-lines, and (c) digitized bank-lines. Landsat image of the year 2009 is displayed in the left panel whereas the right panel shows the image of 2021 collected from Sentinel

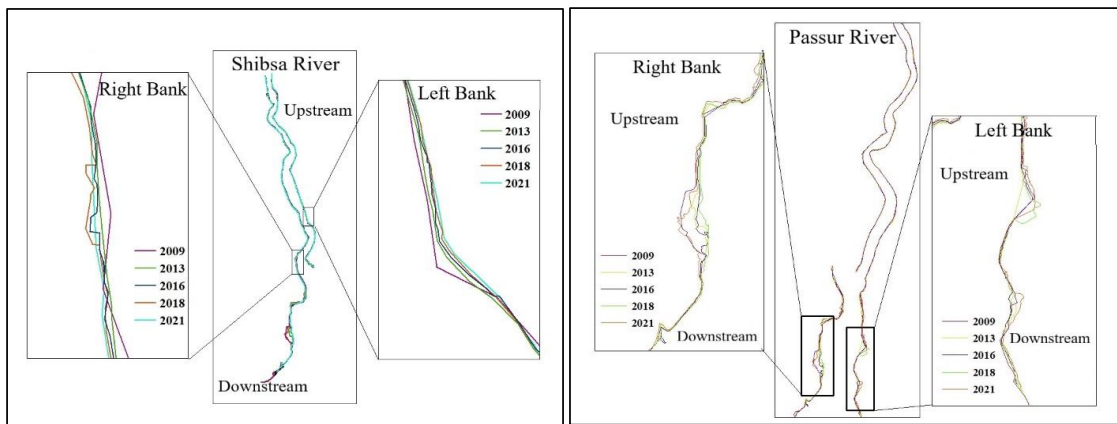


Figure 4: Changing nature of bankline shifting of both right the left bank of the Shibsra (left panel) and Passur (right panel) Rivers between years 2009 and 2021

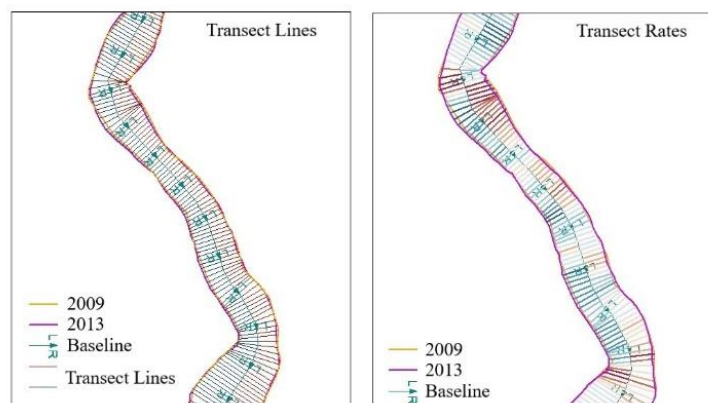


Figure 5: Transects of 150m interval covering the Shibsra River using the DSAS considering a baseline passing through the center of the river. The left panel depicts the transect lines whereas the right panel shows the transect rates after running the DSAS software

iv. Calculation of Net Bankline Movement (NBM)

To analyze the bankline migration patterns, the NBM values were computed using the DSAS tool. The differences between the banklines from various time

periods, including 2009 and 2013, 2013 and 2016, 2016 and 2018, and 2018 and 2021, were calculated. Riverward movement, referred to as accretion, corresponded to banklines moving toward the river, indicated by negative

NBM values. Conversely, landward movement, or erosion, referred to banklines moving away from the river, represented by positive NBM values. The NBM values provided insights into the extent and direction of bankline migration along the transects, allowing for a better understanding of the erosion and accretion processes occurring within the rivers.

v. Critical Zones

Critical zones for erosion and deposition along the left and right banks of the Passur and Shibsra Rivers were identified based on consistent NBM values obtained from the DSAS. The banklines from 2009 to 2021 were compared, and zones exhibiting either landward or riverward migration in at least three out of four comparisons were designated as

critical zones. Non-critical zones were monitored when two or fewer comparisons showed either landward or riverward movements. The transect IDs within these critical zones were selected as observation points for the hydrodynamic model to analyze variations in velocities and bed shear stresses at those erosional and depositional banks. NBM values less than 10 meters were discarded to avoid errors arising from manual digitization. The critical zones and their corresponding transect IDs were used for detailed analysis and model simulations, providing insights into the dynamic nature of bankline movement and identifying areas undergoing changes over time. Table 2 summarizes the location and transect IDs for the critical zones, classified as erosional or depositional zones based on the designated observation points.

Table 2
Location of morphologically critical zones along with transect ID (Zone IDs displayed in the figure)

Zones	Latitude-Longitude	Location	Transect ID
Erosion zone 1 or (a)	89.462°E 22.178°N	Shibsra right bank	216-234
Erosion zone 2 or (d)	89.548°E 22.179°N	Passur right bank	209-227
Erosion zone 3 or (b)	89.525°E 22.039°N	Shibsra left bank	330-346
Erosion zone 4 or (e)	89.577°E 22.061°N	Passur left bank	298-319
Deposition zone 1 or (c)	89.467°E 21.862°N	Passur right bank	483-502
Deposition zone 2 or (f)	89.543°E 21.807°N	Passur left bank	521-525

C. Development of a 2D Hydrodynamic Model

Delft3D Flow model suite was used to better understand how river banks change along with the variation of flows and other hydrodynamic parameters.

i. Model Setup

Delft3D suite was employed to develop a 2D hydrodynamic model covering the Shibsra and Passur Rivers particularly to understand the river bank dynamics and also to provide quantitative predictions. Observation points were carefully selected and depicted in Figure 6(a) along with the land-water boundary, including critical zones as identified from the river bankline analysis through satellite imagery and also to monitor water levels, depths, velocities, bed shear stress, flow directions etc. The domain had around 3,600 grid cells as shown in Figure 6(b), and the grids were orthogonalized to enhance performance while keeping a range of values between 0 and 0.26, as shown in Figure 6(c). The depth data collected in 2019 from a secondary source for both the rivers was used to develop bathymetric variation, as shown in Figure 6(d). The depth variation along the middle reach ranges from 10.7 to 14 meters in the Shibsra River which is 10.7 to 17.9 meters in the Passur. The model simulated hydrodynamic parameters at each computational grid points, with specific grids selected as observation points to analyze velocities and bed shear stress in the critical zones. The model was simulated for 30 days with a time step of 60 seconds. The maximum Courant Number shown in Figure 6(e) was found as 12.85 which falls within the acceptable limit according to the Delft3D manual. The Delft3D hydrodynamic model required various parameters and physical characteristics as input including eddy viscosity, bed resistance coefficients and few other

constants, which are summarized in Table 3. The roughness characteristics, represented by Manning's n , is critical for model calibration and were set to $0.025 \text{ s/m}^{1/3}$ for non-vegetated areas (as used by Haque et al., 2016) and $0.10 \text{ s/m}^{1/3}$ for vegetated areas (also used by Islam et al., 2022) along both banks. The model was forced at the upstream open boundary by discharges collected from a secondary source and at the downstream open boundary by water level collected from available tide records. While the model effectively simulates hydrodynamic parameters such as water levels, velocities, and bed shear stress, it does not explicitly account for salinity variations or the specific turbulence induced by ship movements. The model's focus is on the broader hydrodynamic processes affecting erosion and deposition, rather than these more localized or specific influences.

ii. Model Calibration

Model calibration can be achieved through modifying model parameters. Instead of altering all of the parameters, a trial-and-error technique of simulation of the developed model was used by changing Manning's Roughness Coefficient to an average value. Regression coefficients was calculated to get the best match between observed and simulated data at different observation locations. Calibration was been done for the month of April for Passur river. The calibrated water level variation agrees reasonably well with the field water level at Joymoni station.

iii. Model Validation

Due to the limited availability of observation stations within the study area of Shibsra river, validation was conducted only for Passur river in March. The validated water level variations showed good agreement with the

observed field water level at Joymoni station, indicating that the model could simulate the various scenarios used in this study. In addition, the model performed better during the dry season, with a correlation coefficient (r^2) of 0.7882, as shown in Figure 7.

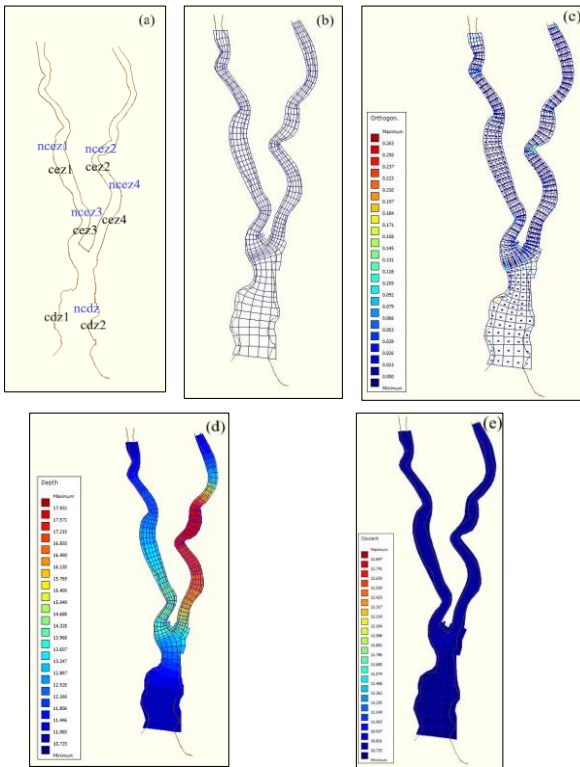


Figure 6: Two-dimensional hydrodynamic model development using Delft3D (a) land-water boundary with observation locations, (b) model grids, (c) grid orthogonality, (d) depth variation and (e) Courant number

Table 3

Hydraulic Parameters used in the model

Parameters	Values Considered
Roughness parameter (Manning's n)	0.025 s/m ^{1/3} and 0.10 s/m ^{1/3}
Horizontal eddy viscosity	1
Water density	1025 kg/m ³

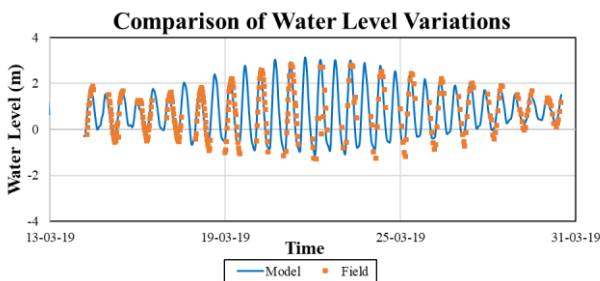


Figure 7: Comparison of model and field water level at Joymoni Station of Passur River covering a spring-neap variation

3. RESULTS AND DISCUSSION

The 2D hydrodynamic model analysis of the Passur and Shibsra rivers provided insights into how these rivers respond to areas of erosion and accretion, which are

considered critically vulnerable zones. The study also included a NBM analysis to assess the dynamics of the riverbanks and their impact on the riverine ecosystem. Moreover, a critical zones analysis was conducted to identify the study area's most susceptible to erosion, accretion, and other environmental stressors, enabling targeted mitigation strategies. Various hydrodynamic parameters i.e. depth-averaged velocity, velocity vectors, and bed shear stress etc. were observed for these critical areas. The variation of velocity and bed shear stress was finally checked in relation to the critical banklines.

A. Net Bankline Movement (NBM) Analysis

The NBM values calculated by the DSAS indicate both riverward (towards the river) and landward (towards the land) migration of the banklines during the studied period, as shown in Figure 8. NBM values ranging from -41.8 to -4.5 meters suggest riverward migration, while values ranging from 40.2 to 1786.1 meters indicate landward migration. NBM values between -4.5 and 10 meters represent a combination of both riverward and landward movement, as shown Figure 8. The right bank of the Shibsra River exhibited predominantly landward movement, as indicated by the positive NBM values projected by DSAS for 2021 compared to 2018. These positive values signify erosion or landward migration, where the bankline moved farther away from the baseline in 2021 relative to its position in 2018. The magnitude of change is depicted by varying colors, with darker colors representing significant bankline shifts and lighter colors indicating slight changes over time (Figure 8).

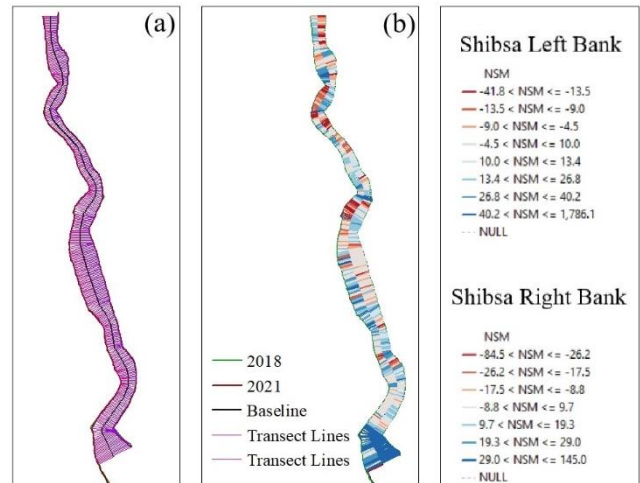


Figure 8: Variation of Net Bank-line Movement (NBM) calculated using DSAS on the Shibsra River between the years 2018 and 2021: (a) transect lines and (b) rate of movement. Net Shoreline Movement (NSM) can be estimated using DSAS which was used in this study for the estimation of NBM

The NBM values computed using the DSAS tool reveal patterns of both riverward and landward migration of the bankline shifts were more pronounced during the period from 2009 to 2013 (represented by the blue color) compared to later years. Additionally, the NBM values exhibit greater magnitudes and increased variability in the downstream regions. The maximum positive and negative NBM values, indicating the largest landward and riverward

movements, respectively, were observed in the downstream sections of the river. Examining Figures 9(c) and 9(d), which depict the bankline movements along the Passur River, a significant variation in both riverward and landward movements can be observed in the downstream region. The transect IDs, ranging from 0 to nearly 582 on the right bank and 0 to 572 on the left bank, increase

sequentially from upstream to downstream, reflecting the elongated nature of the Passur river. Consistent with the observations for the Shibsra river, the maximum positive and negative NBM values, representing the most substantial landward and riverward movements, respectively, were recorded in the downstream sections of the Passur River.

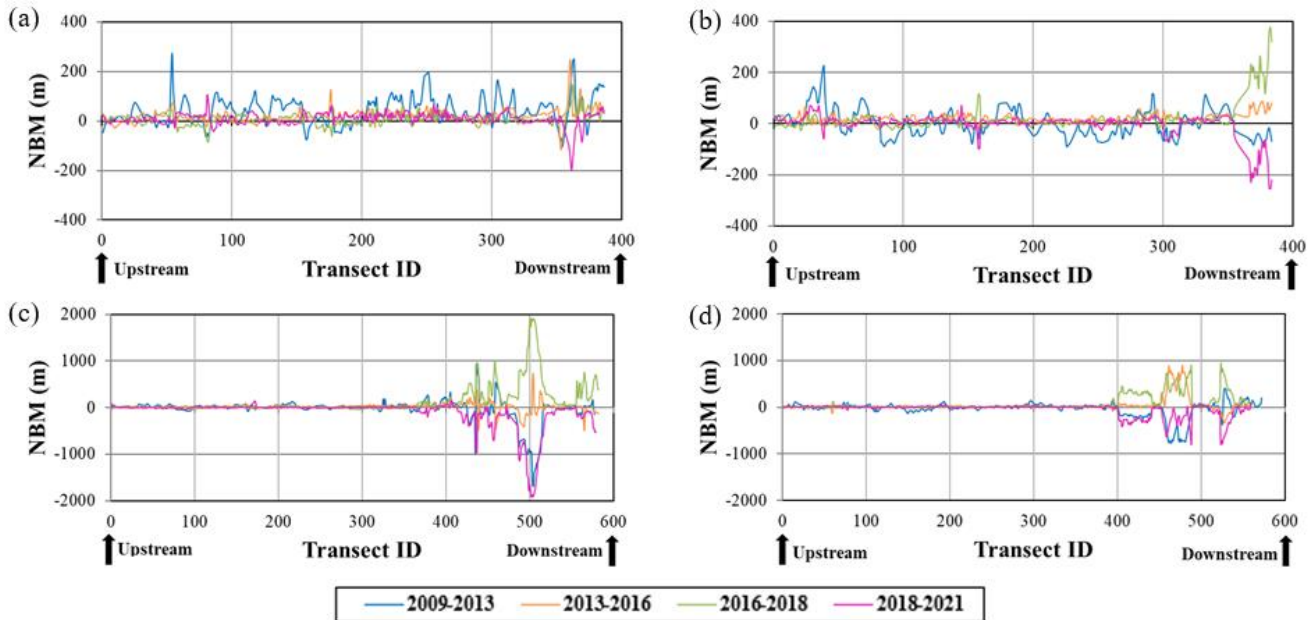


Figure 9: Net Bank-line Movement (NBM) of (a) Shibsra right bank, (b) Shibsra left bank, (c) Passur right bank and (d) Passur left bank

B. Critical Zones Analysis

Figure 10 displays the critical zones for erosion and deposition along both the left and right banks of the Passur and Shibsra rivers. Transect IDs within these critical zones, which are identified based on consistent NBM values, are shown in black and six zones are zoomed in for detailed analysis. In Figure 10(a), the right bank of the Shibsra river is identified as a critical erosion zone, with NBM values ranging from 10 meters to a maximum of 114.88 meters. Figure 10(b) shows the erosion zone for the left bank of the Shibsra river, with NBM values ranging from 10.36 meters to a maximum of 115.24 meters. The deposition zone for the right bank of the Passur river is depicted in Figure 10(c), with NBM values ranging from a minimum of 1773.59 meters to a maximum of 1931.2 meters. Figure 10(d) displays the erosion zone for the right bank of the Passur river, with a maximum NBM value of 126.88 meters. In Figure 10(e), the erosion zone for the left bank of the Passur river is shown, with NBM values ranging from a minimum of 5.79 meters to a maximum of 119.19 meters. Figure 10(f) depicts the deposition zone for the left bank of the Passur river, with the highest NBM value of 942.61 meters and the lowest negative value of 798.51 meters. These critical zones for erosion and deposition provide valuable insights into the dynamics of bankline movement and help to identify areas undergoing significant changes over time. NBM values less than 10 meters were discarded to avoid errors arising from manual digitization.

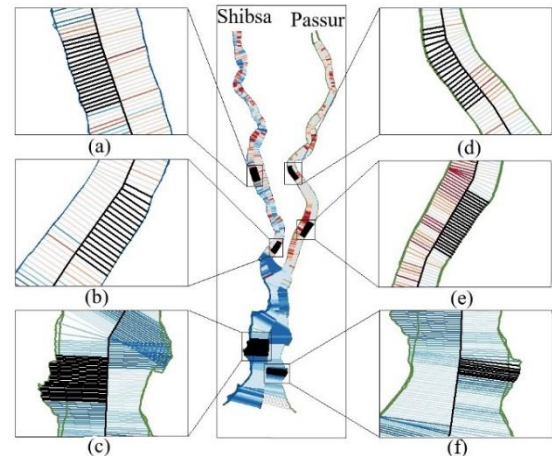


Figure 10: Examples of critical zones of both the Shibsra and Passur rivers where the bank-line movements are significant

Figure 11 provides close-up views of the NBM values plotted against Transect ID for six critical zones. The blue line represents the bankline change from 2009 to 2013, the orange line shows the change from 2013 to 2016, the green line depicts the change from 2016 to 2018, and the pink lines represent the bankline change between 2018 and 2021. Figures 11(a) and 11(b) show continuous erosion in transect IDs 216 to 234 of the Shibsra river's right bank and transect IDs 330 to 346 of the left bank, respectively, for the years 2009-2013, 2013-2016, 2016-2018, and 2018-2021. In Figures 11(c), 11(d), 11(e), and 11(f), critical bankline movements of the Passur river are shown. Figures

11(d) and 11(e) display erosion or landward movement on the right bank and left bank of the Passur river, respectively, in sequential order. In Figures 11(c) and 11(f), critical accretion or riverward movement can be observed in the Passur river based on the NBM values. From the six figures, it is evident that riverward movement occurred in the downstream sections of the rivers, while erosion took place in the mid-portion of the rivers where sharp bends exists. This feature aligns with the expected behavior of a meandering river, where erosion typically occurs on the outer banks of bends, as observed in Figures 11(a), 11(b), 11(d), and 11(e).

C. Non-Hydrodynamic Characteristics

Figure 12 shows a simulated 24-hour tidal cycle covering flood and ebb tide for March 2019. The flood tide is the phase when the tidal current flows inland (flood current),

causing the water level to rise. The ebb tide is the phase when the tidal current flows seaward (ebb current), causing the water level to fall.

Figure 13 displays the variation of velocity vectors during flood or ebb tide. The zoomed-in images provide a better view of the direction of the velocity vectors. During the ebbing period, the currents move seaward, as shown in Figure 13(a). In the Shibsra River, the currents flow from upstream to downstream, while in the Passur River, they flow in the opposite direction, from downstream to upstream. This contrasting behavior suggests the presence of a slack tide, a period of minimal or no current, at the confluence of the two rivers, as shown in Figure 13(b). Additionally, Figure 13(c) illustrates a situation where the currents are moving from downstream to upstream across the entire study region, indicating a flood period.

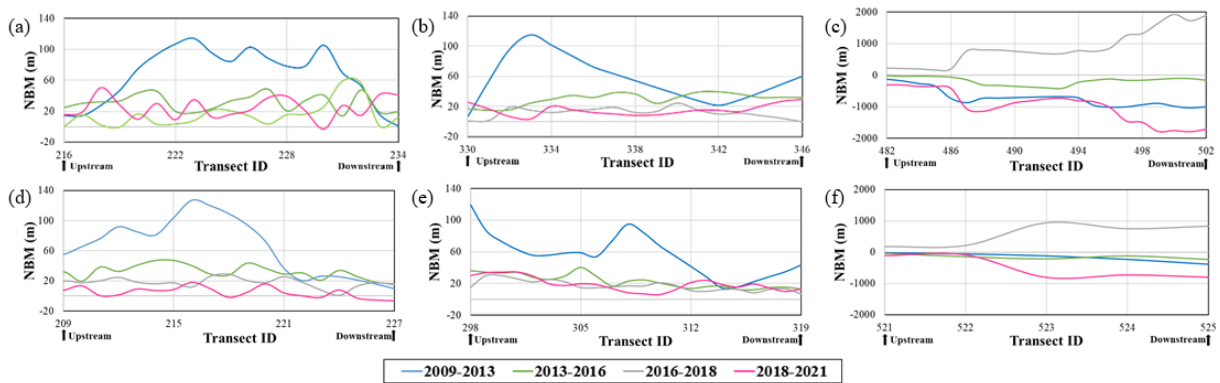


Figure 11: Close-up views of the critical zones: (a) erosion on Shibsra right bank, (b) erosion on Shibsra left bank, (c) accretion on Passur right bank, (d) erosion on Passur right bank, (e) erosion on Passur left bank, and (f) accretion on Passur left bank

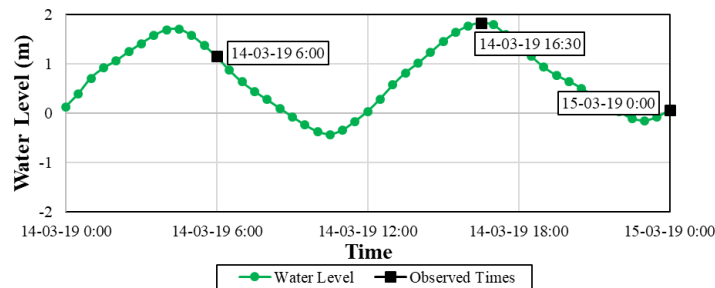


Figure 12: Close-up view of water level variation covering a tidal cycle. Details of water level and velocity variations are shown in the next figure during the highlighted times

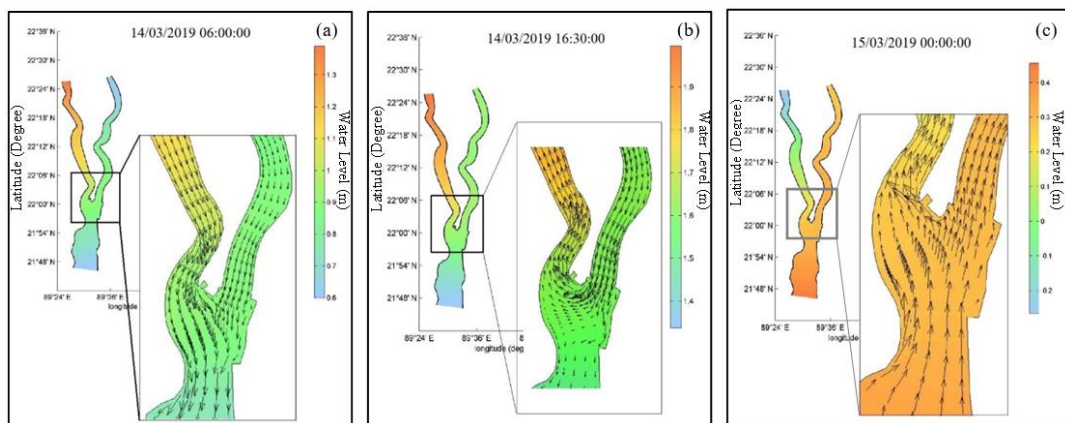


Figure 13: Water level and velocity variation during different tidal conditions: (a) ebb tide, (b) slack tide and (c) flood tide

D. Anthropogenic Factors Influencing River Dynamics

While the study primarily focused on natural hydrodynamic processes, it's important to acknowledge the potential influence of anthropogenic factors on erosion and deposition patterns, particularly in the Passur River (Menezes et al., 2024). The presence of Mongla port and the associated frequent movement of large ships through the Passur River likely contribute to the river's erosion and deposition dynamics (Chakraborty et al., 2024). Ship-induced waves and propeller wash can cause additional stress on riverbanks, potentially accelerating erosion in vulnerable areas (Chakraborty et al., 2022). Furthermore, dredging activities to maintain navigable channels for ship traffic may alter sediment transport patterns (Amanambu & Mossa, 2023). These anthropogenic influences may partially explain some of the differences observed between the Passur and Shibsra rivers in terms of their erosion and deposition characteristics.

E. Comparison of Velocity in Critical and Non-Critical Zones

The results show that water velocities are significantly higher in the critical erosion-prone zones compared to the non-critical areas upstream, as shown in Figure 14(a) and

Figure 14(b). Conversely, the deposition-prone areas exhibit lower water velocities, causing larger particles to settle as the water flow decelerates. The figures show a pattern where erosion occurs upstream and water velocities are high, while deposition takes place downstream, where velocities are comparatively low. Although bed shear stress can be considered as a more reliable predictor of erosion than velocity alone, velocity measurements are more accessible and practical. Therefore, both parameters – water velocity and shear stress – are included in the discussion to provide a comprehensive analysis of the erosion and deposition processes in these critical zones. As seen in Figure 15, Erosion zone 3 is located on the outer edge of a bend and the velocity of water is maximum towards the exterior resulting in erosion of bank lines. The findings align with the understanding that as water slows, larger particles are deposited. Figure 14(a) shows that the velocity is substantially higher in critical erosion-prone zones than in non-critical ones upstream, while frequent deposition downstream indicates that the velocity has reduced. Consequently, the velocity for the depositional zone is less than the velocity in non-critical zone as shown in Figure 14(b).

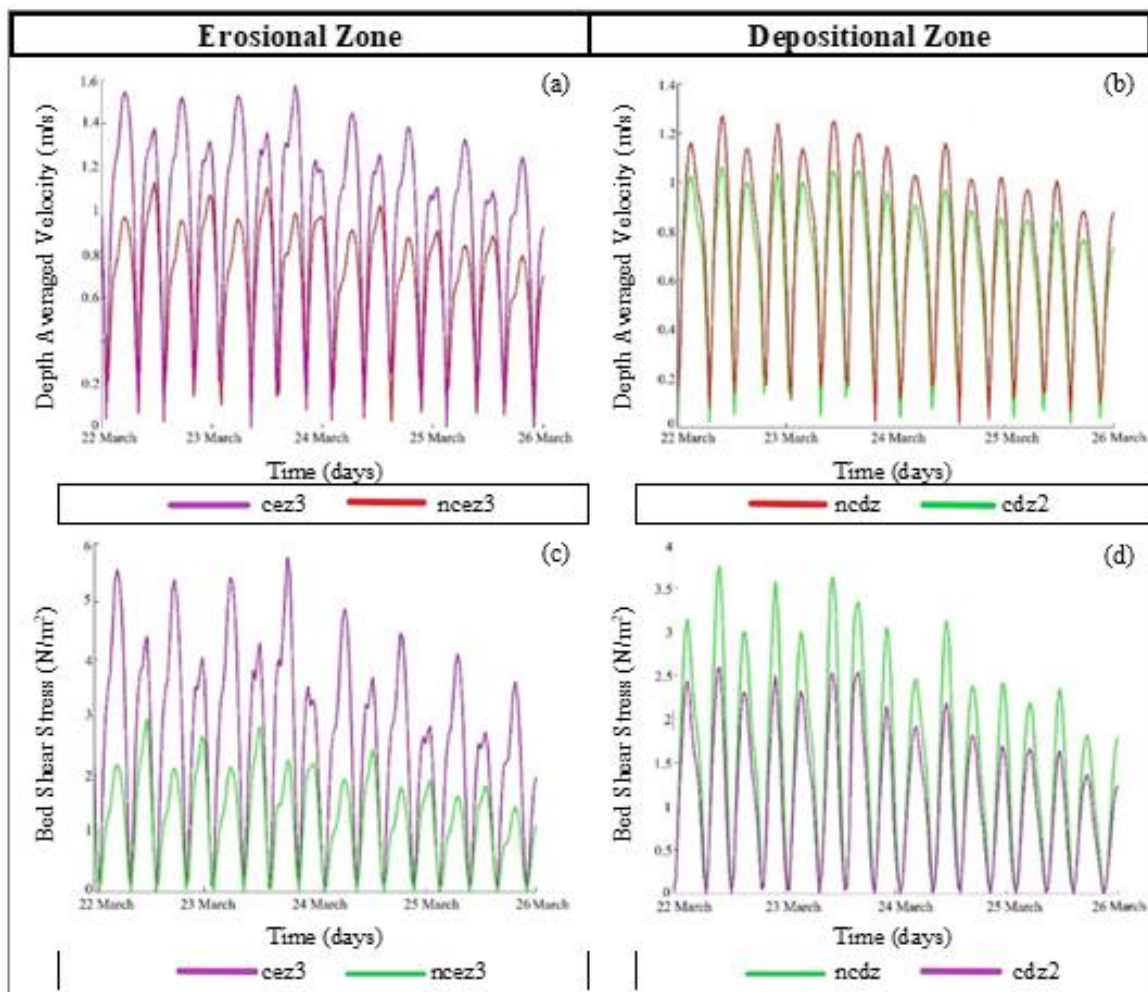


Figure 14: Comparison of velocity and bed shear variation between critical and non-critical zones (a) a critical erosional zone (cez3) and non-critical erosional zone (ncez3), and (b) a critical depositional zone (cdz2) and a non-critical depositional zone (ncdz)

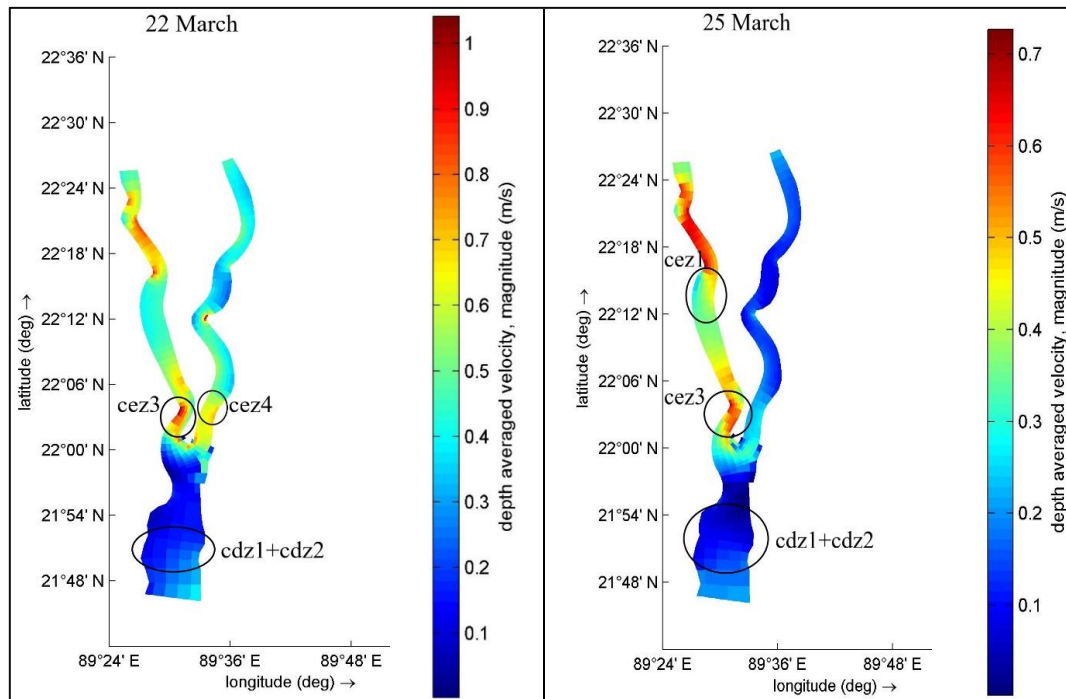


Figure 15: Velocity patterns along with their magnitudes at some critical zones

F. Comparison of Bed Shear Stress in Critical and Non-Critical Zones

The results shown in Figure 14(c) and Figure 14(d) indicate that the bed shear stress values are considerably higher in erosion-prone critical zone compared to non-critical zones. This finding aligns with previous studies (Croad, 1981; Hoffmans & Verheij, 1997; Raudkivi, 1998; Bollaert, 2002; Hoflad *et al.*, 2005; Briaud, 2008) that have examined the contribution of turbulence fluctuations to the erosion process. The higher bed shear stress values in the critical erosion zones can be attributed to the increased shear stress resulting from factors such as higher fluid density, steeper slope, greater water depth, and increased flow velocity. Furthermore, as the channel narrows or the flow velocity increases, the shear stress also rises, leading to higher values in the erosion-prone areas. The comparatively higher shear stress along the outer borders of the bend can directly erode the banks through fluid shear or destabilize the bank's foot or the pool, rendering the bank too steep or high for stability. However, the results also show that as the velocity decreases, the bed shear stress in deposition-prone areas becomes lower than in non-critical zones, which can be explained by the reduced shear stress due to the lower flow velocity (as can be seen from Figure 14).

The present findings align with previous studies conducted in natural environments (Jackson, 1975) and computational models (Ikeda & Parker, 1989; Nelson & Smith, 1989; Sun *et al.*, 2001). The results demonstrate that higher shear stresses and sporadic erosion on the upstream side of the bar can cause the location of the point bar to shift downstream relative to the bend apex. However, the susceptibility to erosion is not solely determined by the magnitude of velocity and shear stress acting on the riverbanks but also depends on the frequency and duration of exposure to high magnitudes exceeding the threshold

value (Avila *et al.*, 2014). Based on these observations, future efforts in model development should focus on enhancing the realism of bank surface erosion in the model to better capture the erosion and deposition dynamics in the Passur and Shibsra rivers.

4. CONCLUSIONS

The present study employed historical image analysis and bankline digitization to investigate erosion and deposition patterns in the Passur and Shibsra rivers. The findings revealed a complex interplay between erosion and deposition processes, with six critical zones identified for landward or riverward bankline shifting. Among these zones, four exhibited predominant erosion tendencies, while two showed notable deposition characteristics. The rivers demonstrated expected hydrodynamic responses, with higher velocities and bed shear stress observed in erosion-prone areas and lower values in deposition-prone areas. The average depth velocity and bed shear stress values are associated with the likelihood of bankline erosion or accretion in the identified critical zones. Higher velocities and bed shear stresses within specific ranges in erosion-prone zones can lead to increased bankline erosion, while lower values within corresponding ranges in deposition-prone zones can promote bankline accretion. These observations align with established geomorphological principles, including the influence of shear stresses on the downstream migration of point bars relative to bend apices. The susceptibility to erosion depends not only on the magnitude of velocity and shear stress acting on the riverbanks but also on the frequency and duration of exposure to high magnitudes exceeding the threshold. Future model development efforts should focus on improving the realism of bank surface erosion simulations to better capture the intricate erosion and deposition dynamics observed in the Passur and Shibsra rivers.

REFERENCES

- Abu Hanipah, A. H., Guo, Z. R., & Zahran, E. S. M. M. (2018). *Hydrodynamic Modeling of a River with Mangrove Forests. 7th Brunei International Conference on Engineering and Technology 2018 (BICET 2018)*. DOI: 10.1049/cp.2018.1511.
- Alam, S., & Matin, M. A. (2013). Application of 2D morphological model to assess the response of Karnafuli River due to capital dredging. *Journal of Water Resources and Ocean Science*, 2(3), 40-48. DOI: 10.11648/j.wros.20130203.13
- Amanambu, A. C., & Mossa, J. (2024). Machine learning insights of anthropogenic and natural influences on riverbed deformation in a large lowland river. *Geomorphology*, 446, 108986. DOI: 10.1016/j.geomorph.2023.108986
- Anam, M. M., Jabir, A. A., & Hasan, G. M. J. (2021). Bank-Line Behaviour of the Main Rivers Located within Sundarbans Using Digital Shoreline Analysis System. *MIST International Journal of Science and Technology*, 9. DOI: 10.47981/j.mijst.09(01)2021.288(11-21)
- Ashraf, M., & Shakir, A. S. (2018). Prediction of River Bank Erosion and Protection Works in a Reach of Chenab River, Pakistan. *Arabian Journal of Geosciences*, 11(7). DOI: 10.1007/s12517-018-3493-7.
- Avila, H., Cuervo, G. H., & Daza, R. (2014). Susceptibility Analysis of River Bank Erosion Based on Exposure to Shear Stress and Velocity Combined with Hydrologic and Geomorphologic Variables. *World Environmental and Water Resources Congress 2014*. DOI:10.1061/9780784413548.154
- Briaud J. L. (2008). Case Histories in Soil and Rock Erosion: Woodrow Wilson Bridge, Brazos River Meander, Normandy Cliffs, and New Orleans Levees. The 9th Ralph B. Peck Lecture, *Journal of Geotechnical and Geoenvironmental Engineering*, 134(10), ASCE, Reston, Virginia, USA.
- Bristow, C. S. (1987). Brahmaputra River: Channel Migration and Deposition. The Society of Economic Paleontologists and Mineralogists (SEPM), *Recent Developments in Fluvial Sedimentology* (SP39), 1987. DOI:10.2110/pec.87.39.0063.
- Chakraborty, M., Sriram, V., & Murali, K. (2022). Impact of the ship waves and tidal forces on the sediment resuspension in inland waterways. *Coastal Engineering Proceedings*, (37), 52-52. DOI: 10.9753/icce.v37.papers.52
- Chakraborty, M., Sriram, V., & Murali, K. (2024). Investigation of ship-induced hydrodynamics and sediment resuspension in a restricted waterway. *Applied Ocean Research*, 142, 103831. DOI: 10.1016/j.apor.2023.103831
- Das, T. K., Halder, S. K., Gupta, I. D., & Sen, S. (2014). River Bank Erosion Induced Human Displacement and Its Consequences. *Living Reviews in Landscape Research*, 8(3), 1-35. DOI: 10.12942/lrlr-2014-3.
- Ghosh, D. & Sahu, A. S. (2018). Problem of River Bank Failure and the Condition of the Erosion Victims: A Case Study in Dhulian, West Bengal, India. *Regional Science Inquiry*, 10(2), 205-214.
- Giri, C., Pengra, B. W., Zhu Z., Singh A., & Tieszen L. L. (2007). Monitoring Mangrove Forest Dynamics of the Sundarbans in Bangladesh and India Using Multi-Temporal Satellite Data from 1973 to 2000. *Estuarine, Coastal and Shelf Science*, 73(1-2), 91-100. DOI: 10.1016/j.ecss.2006.12.019
- Habibullah, M. (1987). Computer Modeling of River Channel Changes in Alluvial Condition. First Interim Report R 02/87, IFCDR, BUET, Dhaka.
- Haque, A., Sumaiya, & Rahman, M. (2016). Flow distribution and sediment transport mechanism in the estuarine systems of Ganges-Brahmaputra-Meghna delta. *International Journal of Environmental Science and Development*, 7(1), 22-30. DOI: 10.7763/IJESD.2016.V7.735
- Hasan, G.M.J., & Matin, N. (2019). Estimation of Areal Changes along the Coastline of Bangladesh due to Erosion and Accretion. *International Journal of Engineering Sciences* 12(3), 111-117. DOI: 10.36224/ijes.120305
- Hasanuzzaman, M., Bera, B., Islam, A. & Shit, P. K. (2021). Estimation and Prediction of Riverbank Erosion Susceptibility and Shifting Rate Using DSAS, BEHI, and REBVI Models: Evidence from the Lower Ganga River in India. <https://doi.org/10.21203/rs.3.rs-1097959/v1>
- Hassan, A., Hoque, I., Huq, P. A. K., Martin, T. C., Nishat, A., & Thorne, C. R. (1997). Defining the banklines of Brahmaputra-Jamuna River using satellite imagery. In *Proceedings of the 3rd International Conference on River Flood Hydraulics*, Oxford, 349-358.
- Hossain, S. & Yeham (2014). A Study on Morphological Change of Meghna River Due to Climate Change by Using GIS Map Analysis. 2nd international Conference on Advances in Civil Engineering 2014 (ICACE-2014), ID: WRE051.
- Ikeda, S., & Parker, G. (1989). River Meandering. *American Geophysical Union: Water Resources Monograph*, 12, 321-378. DOI: 10.1029/WM012
- Islam, M. S. & Wahab, M. A. (2005). A Review on the Present Status and Management of Mangrove Wetland Habitat Resources in Bangladesh with Emphasis on Mangrove Fisheries and Aquaculture. *Hydrobiologia*, 542, 165-190.
- Islam, M. F., Schot, P. P., Dekker, S. C., Griffioen, J., & Middelkoop, H. (2022). Physical controls and a priori estimation of raising land surface elevation across the southwestern Bangladesh delta using tidal river management. *Hydrology and Earth System Sciences*, 26(4), 903-921. DOI: 10.5194/hess-26-903-2022
- Jana, S. (2019). An Automated Approach Estimation and Prediction of Riverbank Shifting for Flood-Prone Middle-Lower Course of the Subarnarekha River, India. *International Journal of River Basin Management*, 1-19. DOI: 10.1080/15715124.2019.1695259.
- Jackson, R. G. (1976). Depositional model of point bars in the lower Wabash River. *Journal of Sedimentary Research*, 46(3), 579-594.
- Kobashi, D., & Mazda, Y. (2005). Tidal flow in riverine-type mangroves. *Wetlands Ecology and Management*, 13, 615-619.
- Laz, O. U. (2012). Morphological Assessment of a Selected Reach of Jamuna River by Using Delft3D Model. M.Sc. Engineering Thesis, Department of Water Resources Engineering, BUET, Dhaka.
- Lotsari, E., Wainwright, D. J., Corner, G. D., Alho, P., and Kayhko, J. (2014). Surveyed and Modelled One-Year Morphodynamics in the Braided Lower Tana River. *Hydrological Processes*, 28(4), 2685-2716. DOI: 10.1002/hyp.9750
- Markham, B. L., Dabney, P. W., Storey, J. C., Morfitt, R., Knight, E., Kvaran, G., & Kenton, L. (2008). Landsat Data Continuity Mission Calibration and Validation. The 17th William T. Pecora Memorial Remote Sensing Symposium, Denver, Colorado.
- Mazda, Y., Kanazawa, N., & Wolanski, E. (1995). Tidal asymmetry in mangrove creeks. *Hydrobiologia*, 295, 51-58.
- Menezes, D. B., Toyama, D., & Bahia, C. B. (2024). Sediment Profiles and Recording the Effects of Anthropogenic Activities. *Sediment Transport Research - Further Recent Advances. IntechOpen*. DOI: 10.5772/intechopen.1001488
- Midha, N. & Mathur, P. K. (2014). Channel Characteristics and Planform Dynamics in the Indian Terai, Sharda River. *Environmental Management*, 53, 120-134.
- Momen, M.A., Uddin, M.E., & Tasnim, N. (2020). Assessment of Bank Erosion and Accretion of Jamuna River Using GIS and Remote Sensing, Conference: 5th International Conference

- on Advances in Civil Engineering (ICACE-2020) at CUET, Chattogram, Bangladesh. 8p.
- Nelson, J. M., & Smith, J. D. (1989). Evolution and Stability of Erodible Channel Beds. *River Meandering*, chapter 11, pp. 321-377, DOI: 10.1029/WM012p0321
- Nicholas, A. (2012). Numerical simulation of morphodynamic diversity in the World's largest rivers. In *EGU General Assembly Conference Abstracts*, 5989.
- Nicholas, A. (2013a). Morphodynamic Diversity of the World's Largest Rivers. *Geology*, 41(4), 475-478. DOI: 10.1130/G34016.1
- Nicholas, A. (2013b). Modelling the Continuum of River Channel Patterns. *Earth Surface Processes and Landforms*, 38(10), 1187-1196. DOI: 10.1002/esp.3431
- Petts, G. E. & Gurnell, A. M. (2005). Dams and Geomorphology: Research Progress and Future Directions. *Geomorphology*, 71, 27-47.
- Rahman, M. M. (2012). Time-series Analysis of Coastal Erosion in The Sundarbans Mangrove. *International Archives of the Photogrammetry, Remote Sensing and Spatial Information Sciences*, 39(B8), 425-429.
- Ramos, J. & Gracia, J. (2012). Spatial-temporal Fluvial Morphology Analysis in the Quelite River: It's Impact on Communication Systems. *Journal of Hydrology*, 412, 269-278. DOI: 10.1016/j.jhydrol.2011.05.007
- Sadeghi, V., Ebadi, H., & Ahmadi, F.F. (2013). A New Model for Automatic Normalization of Multitemporal Satellite Images Using Artificial Neural Network and Mathematical Methods. *Applied Mathematical Modelling*, 37(9), 6437-6445. <https://doi.org/10.1016/j.apm.2013.01.006>
- Sohel, M.I.S., Hore, S.H., Salam, M.A., Hoque, M.A., Ahmed, N., Rahman, M., Khan, M., & Rahman, S. (2021). Analysis of Erosion-Accretion Dynamics of Major Rivers of World's Largest Mangrove Forest using Geospatial Techniques. *Regional Studies in Marine Science*. DOI: 10.1016/j.rsma.2021.101901
- Sun, T., Meakin, P., & Jøssang, T. (2001). A computer Model for Meandering Rivers with Multiple Bed Load Sediment Sizes 2. *Computer simulations: Water Resources Research*, 37, 2243-2258. DOI: 10.1029/2000WR900397.
- Thieler, E. R., Himmelstoss, E. A., Zichichi, J. L. & Ergul, A. (2009). Digital Shoreline Analysis System (DSAS) version 4.0 — An ArcGIS extension for calculating shoreline change. U.S. Geological Survey Open-File Report 2008-1278.
- Uddin, K., Shrestha, B. & Alam, M.S. (2011). Assessment of Morphological Changes and Vulnerability of River Bank Erosion alongside the River Jamuna Using Remote Sensing. *Journal of Earth Science and Engineering*, 1, 29-34.
- Wahid, S.M., Babel, M.S., & Bhuiyan, A.R. (2007). Hydrologic Monitoring and Analysis in the Sundarbans Mangrove Ecosystem, Bangladesh. *Journal of Hydrology*, 332(3-4), 381-395. DOI: 10.1016/j.jhydrol.2006.07.016
- WCMC (2005). Protected Areas Database. UNEP World Conservation Monitoring Centre. 70p.
- Winterbottom, S. J. (2000). Medium and Short-Term Channel Planform Changes on the Rivers Tay and Tummel, Scotland. *Geomorphology*, 34, 195-208.